ELSEVIER

Journal of Nuclear Materials 278 (2000) 37–47

journal of nuclear materials

www.elsevier.nl/locate/jnucmat

Systematics of the thermodynamic properties of trivalent f-elements in a pyrometallurgical bi-phase extraction system

Hajimu Yamana [a,*], Norihira Wakayama [b], Naohiko Souda [b], Hirotake Moriyama [a]

[a] *Research Reactor Institute, Kyoto University, Kumatori-cho, Sennan-gun, Osaka-fu 590-0494, Japan*
[b] *Graduate School of Engineering, Kyoto University, Yoshida, Sakyo-ku, Kyoto-shi 606-8501, Japan*

Received 20 May 1999; accepted 27 August 1999

Abstract

In order to strengthen the comprehensive understanding on the mechanism of the extraction of f-elements in a pyrometallurgical bi-phase extraction system, which is usable for dry-reprocessing of spent nuclear fuels, some thermodynamic quantities related to their affinity to the solvent materials were studied. A reductive extraction system consisting of molten alkaline chloride and liquid Bi and Zn was selected for this purpose, and the excess free energy of tri-chlorides of lanthanides associated with their solution into alkaline chloride molten salt was estimated. The standard Gibbs energy change of formation of diluted liquid alloy of lanthanides with Bi and Zn was discussed with the aid of a semi-empirical model for alloy formation. Their systematic variations along the f-series were studied to elucidate the distribution behaviors.

PACS: 82.60.Lf; 82.60

1. Introduction

The reductive extraction of f-elements between molten chloride and liquid metal deserves an examination as a possible alternative techniques for reprocessing the spent nuclear fuels. Particularly, its usability as a technique for the group separation of actinides and lanthanides is noticeable owing to the high separation factors between lanthanides and actinides achievable in this system [1,2]. Generally, the separation performance of two elements in a pyrometallurgical reductive extraction system using molten chloride mainly depends on the difference of the standard free energy of formation of their chlorides. On the other hand, it is known that the activity coefficients of the elements in the metallic phase and the molten salt phase greatly influence the separation efficiency. The thermodynamic activities of the elements in either phase are mostly controlled by their chemical affinity to the solvent. For instance, in the liquid metal phase, the affinity of metallic states of solute elements to the liquid metals leads to an excess energetic stabilization of the solute metals. Hence, the solutes lose their thermodynamic activities from those of the pure states. A similar effect occurs onto the cationic states in the molten alkaline chloride salt. Thus, in order to evaluate the effectiveness of the separation of lanthanides and actinides by this technique, their thermodynamic activities in both phases will be an important characteristic for study. Therefore, the purpose of this study is to determine and estimate some major thermodynamic quantities related to their affinity to the phases, and to clarify their systematics along the series. By fulfilling these purposes, predictions of the separation behavior of lanthanides and actinides in similar pyrometallurgical separation systems will be feasible.

The thermodynamic activities of elements in the liquids are the reflection of the thermodynamic stabilities of the elements in the liquids, and thus by measuring them, we can obtain the value of standard Gibbs energy change associated with the solution of solutes into the liquids. The thermodynamic activities of metallic

* Corresponding author. Tel.: +81-724 51 2442; fax: +81-724 51 2634.
E-mail address: yamana@hl.rri.kyoto-u.ac.jp (H. Yamana).

0022-3115/00/$ - see front matter
PII: S0022-3115(99)00228-7

f-elements in liquid metals can be directly determined by an electromotive force (EMF) measurement at any temperature [3–6], and some of them have been reported as the standard Gibbs energy changes of the solution of f-elements into liquid metals. In contrast, with respect to their thermodynamic activities in the molten salt phase, it is difficult to directly measure by EMF, especially at higher temperature than about 773 K. This is because there are few reference electrodes to be easily adapted. As a result, there is insufficient data related to the thermodynamic activity of f-elements in the molten salt phase.

From the above points of view, in this study, we describe our trial to estimate the excess free energy of chlorides of trivalent f-elements in the salt phase. By adapting their distribution ratios which were determined in the bi-phase extraction experiments, the excess free energy of trivalent f-elements in the molten salt phase was estimated by using the theoretical relations of related thermodynamic quantities. In addition, the systematic variation of the major thermodynamic quantities along the f-series was discussed.

2. Experimental

The experimental procedures to determine the distribution ratios of lanthanides and actinides in a reductive extraction system have been already reported elsewhere and briefly given here [1,2]. By using radioactive tracers, equilibrium distributions of trivalent lanthanides and actinides were radiochemically determined at 873 and 1073 K in a bi-phase system of molten eutectic mixture of LiCl and KCl (mole ratio of lithium to potassium = 51/49) and liquid Bi or Zn. The 99.9% pure KCl–LiCl mixture was purchased from Anderson Physics Laboratory Engineered Materials and all other reagents used were of analytical grade purchased from Wako Pure Chemicals. All the extraction experiments were performed in a glove box filled with purified Ar the humidity of which was kept <1 ppm. In a typical experiment, 2 mol of LiCl–KCl mixture with 2 mol of Zn or Bi and radioactive solutes were loaded in a sintered alumina crucible and it was heated to a given temperature by an electric furnace. The distribution of the solutes between two phases was controlled by adding a piece of Li–Zn or Li–Bi alloy as a reductant. After achieving an equilibrium by contacting them over 6 h, small portions of both phases were sucked into a stainless steel tube for analysis. All the samples were weighed and their radioactivities were measured by γ-spectrometry (lanthanides) or α-spectrometry (Am and Cm) to determine their concentrations in either phase. Thus the distribution ratio of solutes (D_M) was determined as the ratio of their concentration in metal phase to that in salt phase. The Li concentration in the metal phase sample was determined by atomic absorption spectrophotometry to obtain the distribution ratio of Li (D_{Li}). In this study, all the concentrations of the components were given in the unit of a mole fraction.

3. Results and discussion

3.1. Thermodynamic expression of the extractability

The reductive extraction of trivalent lanthanides by metallic Li is described by Eq. (1)

$$MCl_3(\text{in S}) + 3Li(\text{in B}) \leftrightarrow M(\text{in B}) + 3LiCl(\text{in S}), \quad (1)$$

where M represents trivalent f-elements. In Eq. (1), the salt phase and the metal phase are denoted by S and B, respectively, where B represents Bi or Zn. The brackets mean that the components are not pure solids but are dissolved species in designated phases, and thus, MCl_3(in S) represents the molten chlorides of f-elements dissolved in molten LiCl–KCl. This is considered to be a trivalent cation of M, which is present under a certain interaction with the components or the structure of matrix molten salt. M(in B) represents metallic M as a liquefied alloy with B, which means that M is present as a certain intermetallic complex with B.

The thermodynamic equilibrium constant K of reaction (1) is given by the right-hand side part of Eq. (2), where a denotes the thermodynamic activity of the components which are standardized to those of infinite dilution. In the conditions of the experiments of this study, the concentrations of MCl_3(in S), Li(in B) and M(in B) are low enough that their activities can be approximated by their concentration, and thus it is rewritten by the second part of the equation where γ_{LiCl} is an activity coefficient needed for correcting the high concentration of LiCl(in S). By adapting the relation between K and ΔG^0_{ext}, Eq. (3) is obtained as a function of the distribution ratios D_M and D_{Li} which are defined by [M(in B)]/[MCl_3(in S)] and [Li(in B)]/[LiCl(in S)], respectively. In Eq. (3), ΔG^0_{ext}represents the standard Gibbs energy change of reaction (1).

$$\begin{aligned} K &= \frac{a_{M(\text{in B})} a^3_{LiCl(\text{in S})}}{a_{MCl_3(\text{in S})} a^3_{Li(\text{in B})}} \\ &= \frac{[M(\text{in B})][LiCl(\text{in S})]^3 \gamma^3_{LiCl}}{[MCl_3(\text{in S})][Li(\text{in B})]^3}, \end{aligned} \quad (2)$$

$$\log(D_M/D^3_{Li}) = -3\log\gamma_{LiCl} - \frac{1}{2.3RT}\Delta G^0_{ext}. \quad (3)$$

Therefore, by measuring $\log(D_M/D^3_{Li})$ for every element in the extraction experiments, the value of the right-hand side of Eq. (3) can be determined.

3.2. Results of the extraction experiment

Both in Zn and Bi systems, about 10–20 pairs of $\log D_M$ and $\log D_{Li}$ for some trivalent lanthanides and two trivalent actinides(Am and Cm) were measured at two different temperatures, 873 and 1073 K. The averaged $\log(D_M/D_{Li}^3)$ values of elements were obtained as an intercept of the 3rd-powered linear dependence of $\log D_M$ on $\log D_{Li}$ which were determined by applying the least-square method of curve fitting to the sets of the $\log D_M$ and $\log D_{Li}$ data. A representative example of the obtained relations between $\log D_M$ and $\log D_{Li}$ for La is given as Fig. 1, and all the results of $\log(D_M/D_{Li}^3)$ of trivalent lanthanides and actinides are summarized in Table 1 [1,2].

3.3. Relation of the thermodynamic quantities

The standard Gibbs energy changes of formation of four species of reaction (1) are denoted by $\Delta G_f^0[MCl_3$ in S], ΔG_f^0[Li in B], ΔG_f^0[M in B] and ΔG_f^0[LiCl in S], respectively. These ΔG_f^0 are defined as the standard Gibbs energy changes associated with the formation of infinitely diluted species of them. As indicated by Eq. (4), they are given as the sum of the free energy change of formation of their liquid states and the excess free energy which arises in mixing these liquids with the solvent liquids. In Eq. (4), $\Delta G_f^0[X, \text{liq}]$ represents the standard Gibbs energy change of formation of liquid states of component X.

$$\begin{aligned}
\Delta G_f^0[MCl_3 \text{ in S}] &= [\Delta G_f^0[MCl_3,\ \text{liq}] + \Delta G^{ex}[MCl_3 \text{ in S}],\\
\Delta G_f^0[\text{Li in B}] &= \Delta G_f^0[\text{Li},\ \text{liq}] + \Delta G^{ex}[\text{Li in B}],\\
\Delta G_f^0[\text{LiCl in S}] &= \Delta G_f^0[\text{LiCl},\ \text{liq}] + \Delta G^{ex}[\text{LiCl in S}]. \qquad (4)
\end{aligned}$$

ΔG_{ext}^0 of Eq. (3) is given by the difference in ΔG_f^0 of products and reactants, and hence, substituting Eq. (4) into Eq. (3) yields Eq. (5) which is the basic thermodynamic expression of this study.

$$\begin{aligned}
\log(D_M/D_{Li}^3) = &-\frac{1}{2.3RT}\Delta G_f^0[\text{M in B}]\\
&+\frac{1}{2.3RT}\{\Delta G_f^0[MCl_3,\ \text{liq}] + \Delta G^{ex}[MCl_3 \text{ in S}]\}\\
&+\frac{3}{2.3RT}\{\Delta G_f^0[\text{Li},\ \text{liq}] + \Delta G^{ex}[\text{Li in B}]\}\\
&-\frac{3}{2.3RT}\{\Delta G_f^0[\text{LiCl},\ \text{liq}] + \Delta G^{ex}[LiCl_3 \text{ in S}]\\
&+2.3RT\log\gamma_{LiCl}\}. \qquad (5)
\end{aligned}$$

Among the thermodynamic quantities in Eq. (5), $\Delta G_f^0[MCl_3,\ \text{liq}]$, ΔG_f^0 [LiCl, liq] and ΔG_f^0 [Li, liq] are available from the published database of thermodynamic constants of inorganic substances [7]. Some of the lanthanides have higher melting points than the given temperature of the experiments. In such cases, they were hypothetically treated as super-cooled liquids. ΔG^{ex}[Li in B] was calculated from the reported activity coefficients of Li in Zn [3] and Bi [8], and ΔG^{ex} [LiCl in S] + $2.3RT \log \gamma_{LiCl}$ was also calculated from the reported activity coefficient of LiCl in the eutectic mixture of LiCl–KCl [9]. In Eq. (5), if the values of $\log(D_M/D_{Li}^3)$ are determined by the extraction experiments, two parameters ΔG_f^0 [M in B] and $\Delta G^{ex}[MCl_3$ in S] are left

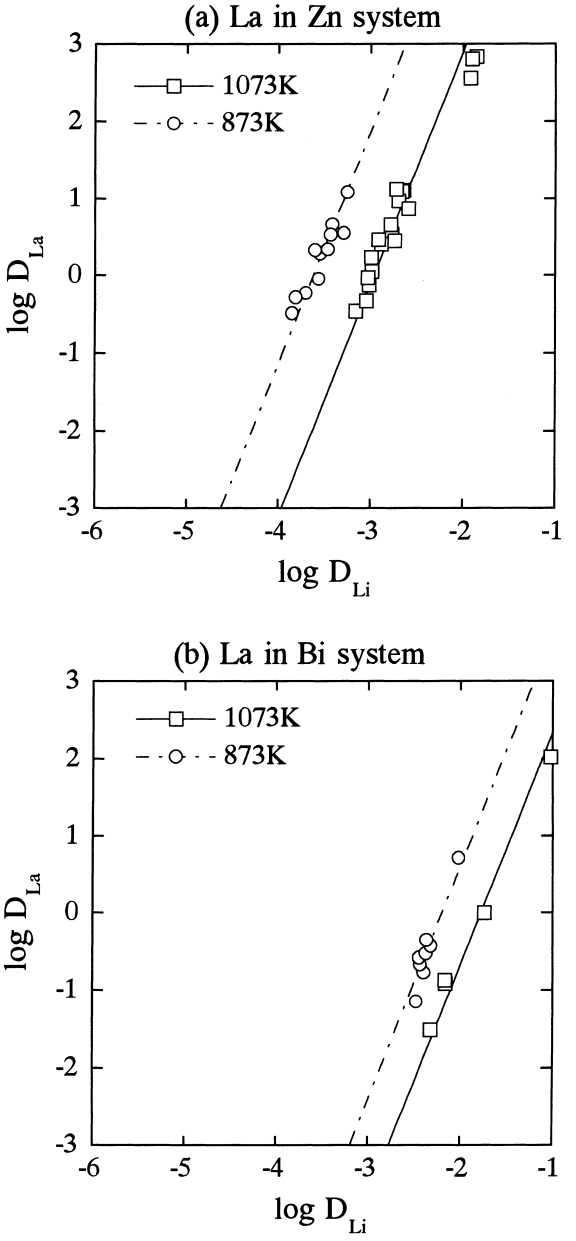

Fig. 1. Linear relations between $\log D_M$ and $\log D_{Li}$ oberved in a bi-phase reductive extraction system of LiCl–KCl eutectic mixture and liquid Zn or Bi.

Table 1
Experimentally determined $\log(D_M/D_{Li}^3)$ of f-elements

	Zn		Bi	
	873 K	1073 K	873 K	1073 K
La	10.879 ± 0.065	8.903 ± 0.061	6.605 ± 0.063	5.328 ± 0.111
Ce	11.197 ± 0.119	9.226 ± 0.072	6.713 ± 0.099	5.668 ± 0.111
Pr	11.578 ± 0.030	9.558 ± 0.056	6.911 ± 0.067	5.664 ± 0.114
Nd	10.935 ± 0.165	8.920 ± 0.243	6.648 ± 0.250	5.608 ± 0.111
Pm				
Sm	6.665 ± 0.112	5.208 ± 0.080	3.492 ± 0.322	3.136 ± 0.080
Eu	5.110 ± 0.100	3.555 ± 0.109	2.617 ± 0.099	1.873 ± 0.128
Gd	10.638 ± 0.351	8.667 ± 0.118	6.478 ± 0.111	5.206 ± 0.125
Tb	11.195 ± 0.103	9.352 ± 0.044	6.389 ± 0.123	5.071 ± 0.125
Dy		9.693 ± 0.085		
Ho	11.010 ± 0.175	9.298 ± 0.091		
Er	10.829 ± 0.197	9.386 ± 0.111		
Tm	10.558 ± 0.074	8.776 ± 0.053	5.708 ± 0.102	5.011 ± 0.114
Yb	6.474 ± 0.196	4.929 ± 0.088	2.568 ± 0.093	1.815 ± 0.095
Lu	10.356 ± 0.080	8.899 ± 0.040		
Am	12.353 ± 0.205	10.309 ± 0.159	9.485 ± 0.202	8.056 ± 0.139
Cm	11.984 ± 0.208	10.040 ± 0.170	9.113 ± 0.150	7.690 ± 0.109

unknown. Thus, by knowing one of these two, the other can be calculated. In this study, reported and estimated values of ΔG_f^0[M in B] were applied to Eq. (5), and ΔG^{ex}[MCl_3 in S] was calculated. In Table 2, quoted values of ΔG_f^0[MCl_3, liq], ΔG_f^0 [LiCl, liq] and ΔG_f^0 [Li, liq] are listed. ΔG^{ex}[Li in B] for Zn and Bi and ΔG^{ex}[LiCl in S]+$2.3RT \log \gamma_{LiCl}$ are also indicated in Table 2.

3.4. Systematic variation of $\Delta G_f^0[MinB]$ of lanthanides

ΔG_f^0[M in B] of lanthanides can be directly measured by the EMF measurement, and some of those for Zn and Bi systems [3–5] have been comprehensively examined and summarized in the literature [3]. These are listed in Table 3. In order to estimate the unreported values of ΔG_f^0[M in B] of lanthanides, systematic variation of ΔG_f^0[M in B] along the lanthanide series is discussed.

$$\Delta H_{sol}[\text{A in B}] = V^{2/3}\frac{2P}{n_b(A)^{-1/3} + n_b(B)^{-1/3}} \times \left[-(\Delta\Phi)^2 + \frac{Q}{P}(\Delta n_b^{1/3})^2 - \frac{R}{P} \right], \quad (6)$$

$$\Delta H_{sol}[\text{A in B}] = V^{2/3} f(n_b(A), n_b(B), \Delta\Phi). \quad (7)$$

According to the Miedema's semi-empirical model [10,11], the enthalpy change of solution of metal A into metal B which is denominated as ΔH_{sol}[A in B] is given by Eq. (6), where V is the molar volume of metal A, n_b(A) and n_b(B) are electron density at the boundary of Wigner–Seitz cell, $\Delta\Phi$ is the difference of electronegativities between A and B, and P, Q, R are specific con-

Table 2
Related thermodynamic quantities applied

	ΔG_f^0[MCl_3, liq][a] (kJ/mol)	
	873 K	1073 K
La	−845.2	−810.0
Ce	−832.4	−794.6
Pr	−834.6	−799.0
Nd	−822.3	−787.4
Pm	–	–
Sm	−675.2	−647.9
Eu	−661.4	−633.2
Gd	−795.8	−760.6
Tb	−784.4	−749.3
Dy	−777.2	−740.4
Ho	−783.9	−746.2
Er	−774.4	−736.3
Tm	−768.6	−730.5
Yb	−645.8	−618.3
Lu	−780.4	−748.3
Am	−782.0	−737.1
Cm	−778.3	−733.3
ΔG_f^0[LiCl, liq][a]	−338.6	−326.8
ΔG_f^0[Li, liq][a]	−1.8	−1.8
ΔG_f^0[Li in Bi][b]	−69.0	−31.8
ΔG_f^0[Li in Zn][c]	−31.8	−68.3
ΔG_f^0[LiCl in S] + $2.3RT\gamma_{LiCl}$[d]	−2.2	−2.2

[a] Ref. [7].
[b] Ref. [8].
[c] Ref. [3].
[d] Ref. [9].

Table 3
ΔG_f^0[M in B] of trivalent lanthanides applied and estimated in this study

	ΔG_f^0[M in Bi][a,b] (kJ/mol)		ΔG_f^0[M in Zn][a,b] (kJ/mol)	
	873 K	1073 K	873 K	1073 K
La	−197.6	−194.4	−154.5	−134.8
Ce	−184.1	−176.4	−149.0	−129.5
Pr	−179.8	−168.6	−138.1	−114.3
Nd	−180.1	−172.8	−149.9	−128.4
Pm	(−170.8)	(−164.3)	(−136.0)	(−119.1)
Sm	(−167.7)	(−161.3)	(−133.6)	(−117.4)
Eu	(−167.2)	(−160.7)	(−133.2)	(−117.1)
Gd	−168.0	−163.2	(−132.4)	(−116.2)
Tb	(−158.9)	(−152.5)	(−126.8)	(−112.6)
Dy	(−154.7)	(−148.4)	(−123.6)	(−110.3)
Ho	(−151.6)	(−145.3)	(−121.1)	(−108.6)
Er	−143.8	−139.1	−114.3	−106.4
Tm	(−143.3)	(−137.1)	(−114.7)	(−104.1)
Yb	(−141.2)	(−135.0)	(−113.1)	(−103.0)
Lu	(−133.2)	(−132.5)	(−111.1)	(−101.6)

[a] Ref. [3].
[b] Brackets: estimated in this study.

stants. By introducing a new factor f which encompasses all other terms than $V^{2/3}$, the right-hand side of Eq. (6) yields Eq. (7). The values of related parameters for lanthanides, which are necessary for Miedema's calculation are listed in Table 4 [10]. In Table 4, it is to be noted that the variation of f over the lanthanide series is not so large that f can be roughly approximated to be constant. Consequently, calculated ΔH_{sol}[M in B] for lanthanides approximately shows a linear dependency on $V^{2/3}$, which can be clearly seen in Fig. 2. On the other hand, according to the reported temperature dependence of ΔG_f^0[M in B] [3], associated entropy change is expected to have less contribution to the free energy change and does not largely vary along the series. Therefore, ΔG_f^0[M in B] for lanthanides is expected to show a similar close-to-linear relation reflecting the variation of ΔH_{sol}[M in B]. Actually, the reported ΔG_f^0[M in B] of lanthanides for liquid Zn and Bi which

Table 4
Parameters for Miedema's semi-empirical model[a]

	$V^{2/3}$ [b] ($cm^2/mol^{2/3}$)	Φ[b] (V)	$n_b^{1/3}$[b] ($du^{1/3}$)[c]	f	
				Bi	Zn
La	7.98	3.17	1.18	−30.7	−21.4
Ce	7.76	3.18	1.19	−30.5	−21.6
Pr	7.56	3.19	1.20	−30.2	−21.8
Nd	7.51	3.19	1.20	−30.2	−21.8
Pm	7.43	3.19	1.21	−30.2	−22.2
Sm	7.37	3.20	1.21	−29.9	−21.9
Eu	7.36	3.20	1.21	−29.9	−21.9
Gd	7.34	3.20	1.21	−29.9	−21.9
Tb	7.20	3.21	1.22	−29.6	−22.1
Dy	7.12	3.21	1.22	−29.6	−22.1
Ho	7.06	3.22	1.22	−29.4	−21.8
Er	6.98	3.22	1.23	−29.3	−22.1
Tm	6.90	3.22	1.23	−29.3	−22.1
Yb	6.86	3.22	1.23	−29.3	−22.1
Lu	6.81	3.22	1.24	−29.2	−22.5
Bi	7.20	4.15	1.16		
Zn	4.38	4.10	1.32		

[a] $P = 12.3$; $Q/P = 0.944$; $R/P = 0.715$ for Zn, 1.175 for Bi.
[b] Ref. [11].
[c] $du = 6 \times 10^{22}$ electrons/cm^3.

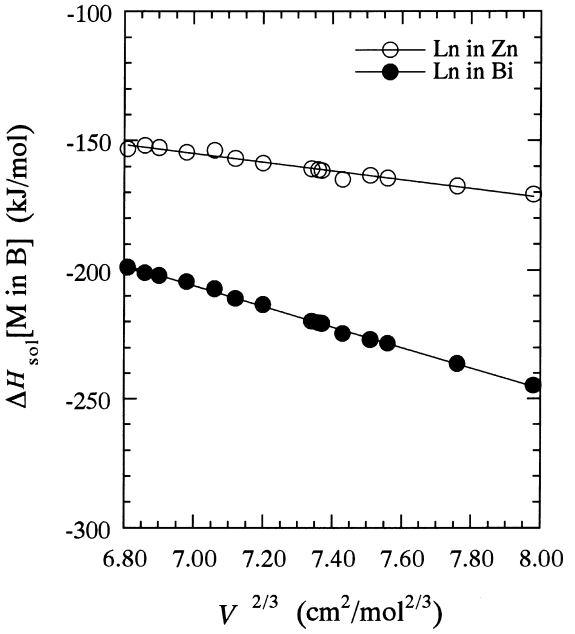

Fig. 2. Calculated enthalpy change of solution of lanthanides into liquid metals by Miedema's semi-empirical model (Dependence on the molar volume) [10,11].

are plotted vs $V^{2/3}$ in Fig. 3 showed close-to-linear relation vs $V^{2/3}$ [3]. Therefore, the values of ΔG_f^0[M in B] of elements, which have not been measured can be estimated by the linear lines of Fig. 3 as a function of $V^{2/3}$ listed in Table 3. The bracketed numbers in Table 3 are the estimated ones by this systematics. The fitted linear relations for liquid Zn at 873 and 1073 K, and for liquid Bi at 873 and 1073 K are respectively given by the following equations which are given in kJ/mol unit. The degree of the reliability of these equations is shown by the errors which are the standard error of estimate of ΔG_f^0[M in B] on $V^{2/3}$.

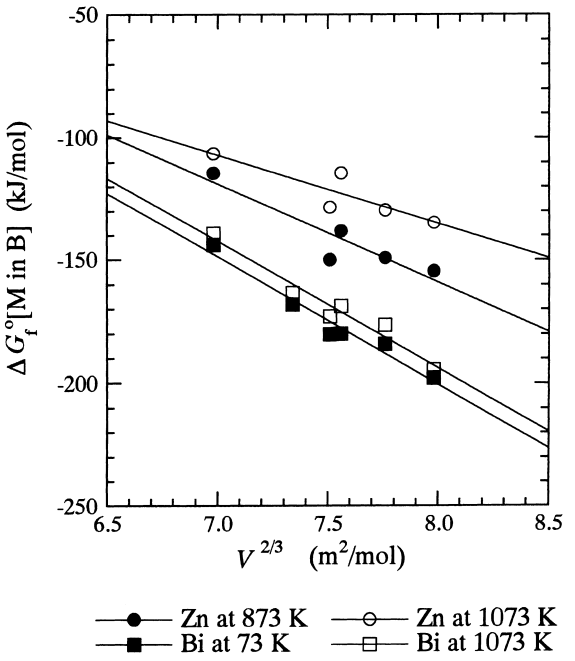

Fig. 3. Linear dependence of reported ΔG_f^0[M in B] of lanthanides on $V^{2/3}$ [3].

$$\Delta G_f^0[\text{M in Zn}]_{873\ \text{K}} = 162.6 - 40.2V^{2/3} \quad \pm 5.5, \tag{8}$$

$$\Delta G_f^0[\text{M in Zn}]_{1073\ \text{K}} = 90.1 - 28.2V^{2/3} \quad \pm 5.0, \tag{9}$$

$$\Delta G_f^0[\text{M in Bi}]_{873\ \text{K}} = 214.5 - 51.9V^{2/3} \quad \pm 3.3, \tag{10}$$

$$\Delta G_f^0[\text{M in Bi}]_{1073\ \text{K}} = 217.5 - 51.4V^{2/3} \quad \pm 3.4. \tag{11}$$

3.5. Systematic variation of $\Delta G^{ex}[MCl_3$ in $S]$

By adapting $\log(D_M/D_{Li}^3)$, $\Delta G_f^0[MCl_3, \text{liq}]$, ΔG_f^0[LiCl, liq], ΔG_f^0[Li, liq], ΔG^{ex}[Li in B], ΔG^{ex}[LiCl in S]$+2.3RT\log\gamma_{LiCl}$, and ΔG_f^0[M in B] to Eq. (5), $\Delta G^{ex}[MCl_3$ in S] for some lanthanides was calculated. The calculated values of $\Delta G^{ex}[MCl_3$ in S] are listed in Table 5. The values of $\Delta G^{ex}[MCl_3$ in S] of lanthanides at two temperatures range from ca. -14 to -90 kJ/mol, which implies the presence of a quite strong chemical stabilization of trivalent cations in the molten chloride phase. In Table 5, it should be noted that $\Delta G^{ex}[MCl_3$ in S] obtained from two independent experimental systems (Zn and Bi) agree quite well, which suggests that this method of estimating $\Delta G^{ex}[MCl_3$ in S] from the distribution ratios is quite successful.

In order to deduce the mechanism of this stabilization of lanthanide cations in the molten salt phase, the dependence of $\Delta G^{ex}[MCl_3$ in S] on the size of the lanthanide cations is discussed. Because we do not have any detailed information on the distance of the nearest neighbor ions from the lanthanides in the molten alkaline chloride matrix, we used the crystalline ionic radius of lanthanide as an index which reflects semi-quantitatively the distance to the nearest neighbor elements. The ionic radii of the elements used are those of tri-positive cations under coordination number 6 [12]. In Figs. 4 and 5, they are plotted vs the inverse of lanthanide's ionic radius. In Figs. 4 and 5, the elements showed a roughly monotonic decrease on $1/R$ except for Pr and Lu which showed certain discrepancies to the same direction from the lines. The linear tendency over the majority of the elements suggests that the stabilization of lanthanide tripositive cations presumably has an inverse dependence on the ionic size. Regarding with the large discrepancies of Pr and Lu from other majority elements which can also be numerically seen in Table 5, we will have to

Table 5
Estimated excess free energy of lanthanide tri-chlorides in LiCl–KCl eutectic mixture[a]

	$1/R$	$\Delta G^{ex}[MCl_3$ in S] at 873 K (kJ/mol)		Most probable line at 873 K (kJ/mol)	$\Delta G^{ex}[MCl_3$ in S] at 1073 K (kJ/mol)		Most probable line at 1073 K (kJ/mol)
		Bi system	Zn system		Bi system	Zn system	
La	0.97	-52.2 ± 4.1	-49.2 ± 3.3	-49.3 ± 4.3	-51.8 ± 4.5	-37.1 ± 3.0	-41.4 ± 6.3
Ce	0.99	-49.8 ± 4.0	-51.3 ± 3.6	-54.3 ± 4.3	-42.2 ± 4.2	-40.6 ± 3.0	-46.4 ± 6.3
Pr	1.01	-39.9 ± 3.8	-31.9 ± 2.8		-30.1 ± 4.1	-14.1 ± 2.6	
Nd	1.02	-56.9 ± 5.5	-66.6 ± 4.1	-60.7 ± 4.3	-47.0 ± 4.1	-52.9 ± 5.6	-52.9 ± 6.3
Pm	1.03			-64.0 ± 4.3			-56.1 ± 6.3
Sm	1.04						
Eu	1.06						
Gd	1.07	-74.1 ± 3.8	-80.6 ± 8.0	-72.3 ± 4.3	-72.5 ± 4.2	-73.0 ± 5.5	-64.4 ± 6.3
Tb	1.08	-77.9 ± 3.9	-77.1 ± 5.7	-76.4 ± 4.3	-75.9 ± 4.3	-66.4 ± 5.0	-68.5 ± 6.3
Dy	1.10			-79.5 ± 4.3		-66.0 ± 5.3	-71.6 ± 6.3
Ho	1.11		-75.1 ± 6.2	-82.7 ± 4.3		-66.6 ± 5.3	-74.8 ± 6.3
Er	1.12		-80.7 ± 4.0	-85.9 ± 4.3		-72.4 ± 3.1	-78.0 ± 6.3
Tm	1.14	-89.5 ± 3.7	-91.5 ± 5.6	-88.9 ± 4.3	-80.5 ± 4.1	-88.5 ± 5.1	-81.0 ± 6.3
Yb	1.15						
Lu	1.16		-79.4 ± 5.6			-65.7 ± 5.0	

	$\Delta G^{ex}[MCl_3$ in S] – ΔG_f^0[M in B] (kJ/mol)	
	Am	Cm
Bi at 873 K	130.3	120.3
Bi at 1073 K	125.8	114.5
Zn at 873 K	66.8	56.9
Zn at 1073 K	53.7	44.5

[a] For Am and Cm, because ΔG_f^0[M in B] is unknown only $\Delta G^{ex}[MCl_3$ in S] – ΔG_f^0[M in B] was determined.

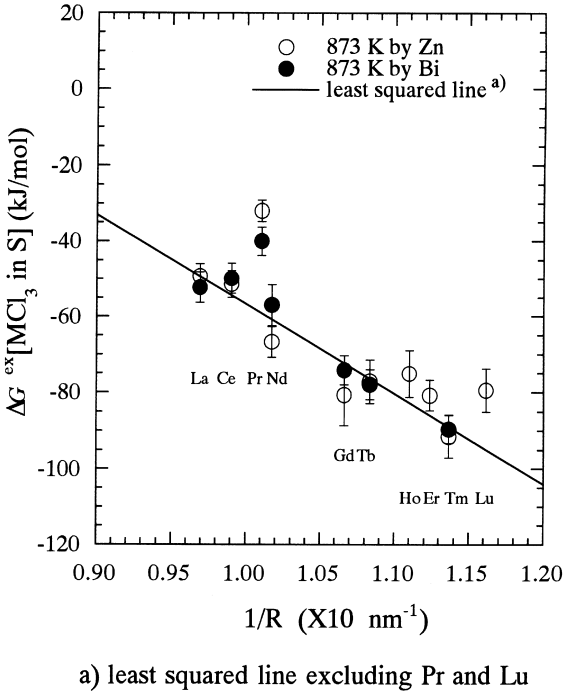

Fig. 4. $\Delta G^{ex}[MCl_3$ in S] of lanthanides derived from experimentally determined distribution ratios and reported thermodynamic quantities (873 K).

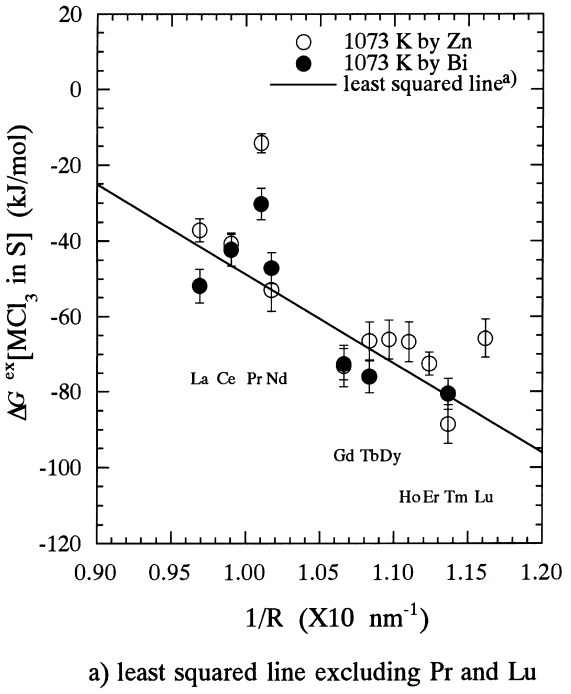

Fig. 5. $\Delta G^{ex}[MCl_3$ in S] of lanthanides derived from experimentally determined distribution ratios and reported thermodynamic quantities (1073 K).

check their reason. Further careful study will be needed in view of the presence of experimental errors, the error of the reported ΔG_f^0[M in B], as well as the possible presence of the some substantial chemical irregularities for these elements.

Most probable chemical potential of this type is of the coulombic interaction between surrounding ions. The following two types of electrostatic mechanisms of stabilization can be presumed, (a) electrostatic potential by the reciprocal coulombic effect in the quasi-lattice structure of chloride salt, and (b) formation of a complex of lanthanide by the coordination of other ions particularly by Cl^-. The mechanism (a) must have a certain role in the total stabilization to some extent, however, the unexpectedly deep stabilization energy observed also implies the presence of mechanism (b). Further study will be needed to elucidate the total mechanism of the stabilization of lanthanide cations in the salt phase.

In Figs. 4 and 5, the most probable lines representing the linear relations of $\Delta G^{ex}[MCl_3$ in S] and $1/R$ were determined by applying the least square fitting to the data points excluding Pr and Lu. It should be noted that the slope of the lines for two different temperatures are almost identical, and thus the lines are approximated by the following equations for 873 and 1073 K, respectively.

$$\Delta G^{ex}[MCl_3 \text{ in S}] = 180.1 - 236.7 \cdot 1/R \quad \pm 4.3, \tag{12}$$

$$\Delta G^{ex}[MCl_3 \text{ in S}] = 188.0 - 236.7 \cdot 1/R \quad \pm 6.3. \tag{13}$$

The difference of $\Delta G^{ex}[MCl_3$ in S] between two different temperatures gives information of the corresponding standard enthalpy change ($\Delta H^{ex}[MCl_3$ in S]) and entropy change ($\Delta S^{ex}[MCl_3$ in S]). Because of the scatter of the data of $\Delta G^{ex}[MCl_3$ in S] in Figs. 4 and 5, by the direct use of these points, we obtain rather scattered $\Delta H^{ex}[MCl_3$ in S] as plotted by the dot circles in Fig. 6. Owing to the error associated with the $\Delta G^{ex}[MCl_3$ in S] estimated, obtained $\Delta H^{ex}[MCl_3$ in S] has so large an error that a quantitative discussion is difficult. $\Delta H^{ex}[MCl_3$ in S] can be derived from the difference of the most probable lines of Eqs. (12) and (13) for 873 and 1073 K, which is shown by the solid line and open squares in Fig. 6. $\Delta H^{ex}[MCl_3$ in S] obtained by these lines also accompanies relatively large error along them owing to the errors of the lines. The parallel lines for two different temperatures imply that the temperature dependence of $\Delta G^{ex}[MCl_3$ in S] is identical for every lanthanide, which provides a common $\Delta S^{ex}[MCl_3$ in S] for the series, 39.4 J/mol. In Table 6, estimated $\Delta H^{ex}[MCl_3$ in S] and $\Delta S^{ex}[MCl_3$ in S] are listed. Despite the presence of the large errors, in Fig. 6, we can see a rough dependence of $\Delta H^{ex}[MCl_3$ in S] on $1/R$, which presumably governs the systematic dependence of

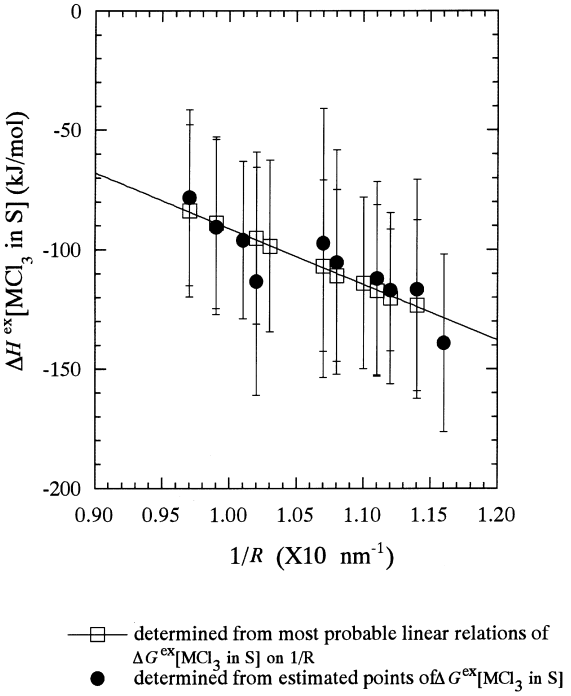

Fig. 6. $\Delta H^{ex}[MCl_3$ in S] of lanthanides estimated from the temperature dependency of $\Delta G^{ex}[MCl_3$ in S].

$\Delta G^{ex}[MCl_3$ in S] on $1/R$. As a result of the consideration on the lanthanides, we can semi-quantitatively consider that the variation of the entropy change along the lanthanide series is small, and that the variation of $\Delta G^{ex}[MCl_3$ in S] along the series is largely dependent on the variation of $\Delta H^{ex}[MCl_3$ in S] which presumably has a significant dependence on the ionic radius of the lanthanides.

$\Delta G^{ex}[MCl_3$ in S] of Am and Cm were unable to be determined in this experiment because their ΔG_f^0[M in B] had not been reported. Therefore, for these two actinides, only the difference of $\Delta G^{ex}[MCl_3$ in S] from ΔG_f^0[M in B] was determined and listed in Table 5.

3.6. Systematic correlation of the thermodynamic quantities

As discussed in the previous section, $\Delta G^{ex}[MCl_3$ in S] becomes more negative with decreasing ionic radius, which means that smaller trivalent cations of lanthanides gain more stabilization in the salt phase. In contrast to this, ΔG_f^0[M in B] becomes more negative with increasing size of the metallic cells of lanthanides, i.e., metallic radius. Their monotonic variations along the 4f-series suggest that the chemical interactions between lanthanides and solvents are simply size-dependent. It presumably implies that 4f-electrons do not play a specific role in the chemical bonding with the solvent components in either phase, except for their role to cause the size-reduction which is well known as the lanthanide-contraction. In other words, either in the cationic state or metallic state, 4f-orbital seems to be deeply localized.

In Fig. 7, for every element studied at 873 K, the correlation between $\Delta G^{ex}[MCl_3$ in S] and ΔG_f^0[M in B] is shown. $\Delta G^{ex}[MCl_3$ in S] shows inverse proportion to ΔG_f^0[M in B] in Zn and Bi systems. In both systems, Pr showed exceptional singularity from the rough correlation lines reflecting its singularity in $\Delta G^{ex}[MCl_3$ in S]. Fig. 7 is convenient to understand the balance of the

Table 6
Estimated $\Delta H^{ex}[MCl_3$ in S] and $\Delta S^{ex}[MCl_3$ in S]

	$1/R$	From estimated lines of $\Delta G^{ex}[MCl_3$ in S]		From estimated points of $\Delta G^{ex}[MCl_3$ in S]	
		$\Delta H^{ex}[MCl_3$ in S] (kJ/mol)	$\Delta S^{ex}[MCl_3$ in S] (J/mol)	$\Delta H^{ex}[MCl_3$ in S] (kJ/mol)	$\Delta S^{ex}[MCl_3$ in S] (J/mol)
La	0.97	-83.7 ± 35.9	−39.4	-78.1 ± 36.7	−31.4
Ce	0.77	-88.7 ± 35.9	−39.4	-90.4 ± 36.7	−45.7
Pr	1.01			-95.9 ± 32.9	−68.8
Nd	1.02	-95.1 ± 35.9	−39.4	-113.1 ± 47.7	−58.9
Pm	1.03	-98.4 ± 35.9	−39.4		
Sm	1.04				
Eu	1.06				
Gd	1.07	-106.7 ± 35.9	−39.4	-97.1 ± 56.4	−22.7
Tb	1.08	-110.8 ± 35.9	−39.4	-105.1 ± 47.0	−31.7
Dy	1.10	-113.9 ± 35.9	−39.4		
Ho	1.11	-117.0 ± 35.9	−39.4	-111.9 ± 40.5	−42.3
Er	1.12	-120.3 ± 35.9	−39.4	-116.8 ± 25.4	−41.4
Tm	1.14	-123.3 ± 35.9	−39.4	-116.5 ± 46.0	−29.8
Yb	1.15				
Lu	1.16			-138.9 ± 37.3	−68.3

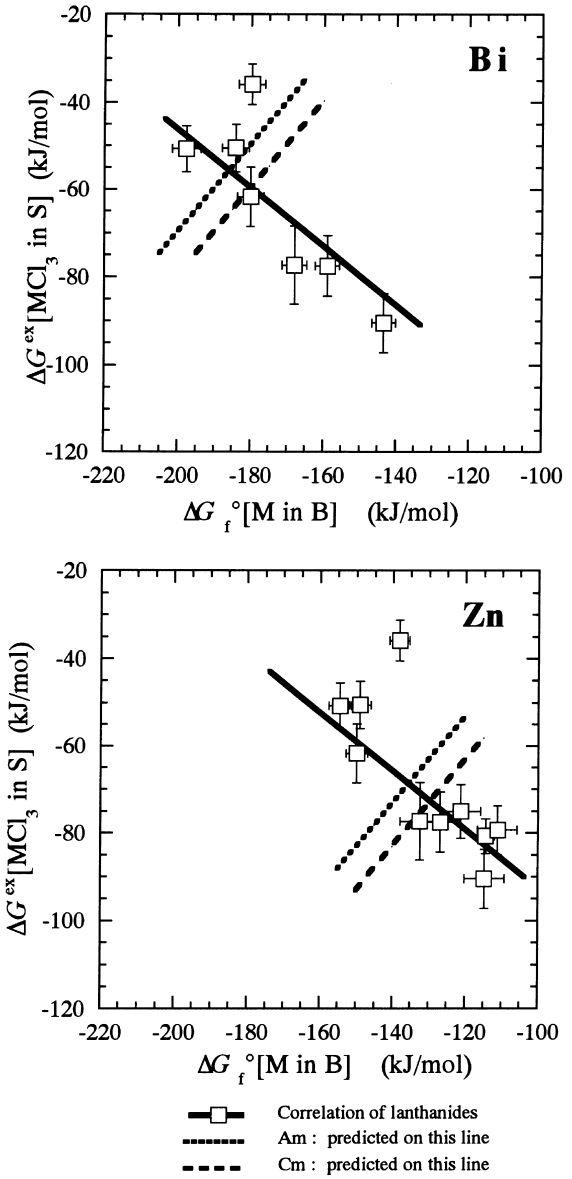

Fig. 7. Correlation between ΔG_f^0 [M in B] and $\Delta G^{ex}[MCl_3$ in S] (873 K).

affinities of elements to two phases, which helps us to evaluate their distribution behaviors. With respect to the elements being located in the upper-left side of Fig. 7, their metallic states of the elements are more favored by the liquid metal phases than the chlorides are favored by the molten salt phase and, hence, there arises an additional force to distribute them to the metallic phase rather than to the salt phase. In contrast, those in the bottom-right side have similar degree of affinity to both phases which are to be canceled out in the extraction distribution and, thus, the distribution of the heavier lanthanides is likely to be only governed by the formation free energy changes of their chlorides. Because of the lack of the data of ΔG_f^0[M in B] for Am and Cm, their $\Delta G^{ex}[MCl_3$ in S] was not able to be determined in this study. Instead, only the difference of the two parameters was estimated for these elements as listed in Table 5, and their possible correlation is indicated in Fig. 7 by the dotted lines on which Am and Cm should show their correlation points.

The correlation lines of lanthanides for Zn and Bi systems are characterized by the large difference in their horizontal locations in the figures. It indicates relatively stronger affinity of Bi to lanthanides than Zn. In Miedema's interpretation above, this is due to the difference of the factor f of Eq. (7) which largely depends on the value of constant term R/P which is specific to different metals. R/P is a factor to correct the presence of an additional bonding which is specific to the selected pair of metals, and, it is considered to be the appearance of an enhanced metallic bonding caused by the hybridization of lanthanides' d-orbital with bismuth's p-orbital. In this context, the difference of the location of Am and Cm relative to the lanthanides deserves special interest because it implies the different feature of the actinides relative to the lanthanides. In the Bi system, the dotted lines of Am and Cm representing possible combination of their $\Delta G^{ex}[MCl_3$ in S] and ΔG_f^0[M in B] are located at the left-side of the correlation lines of lanthanides. It means that, in comparison with the case of Zn system, Am and Cm make relatively stronger bonding with Bi than lanthanides do, and they are likely to act like lighter lanthanides. It is natural to presume that the stronger affinity of actinides to Bi is attributable to the deeper hybridization of the 5f-orbital with the p-orbital of Bi.

4. Conclusion

Based on the experimentally determined distribution ratios of trivalent lanthanides and actinides in the pyrometallurgical reductive extraction system, some thermodynamic quantities related to their affinity to the solvent materials were studied. With respect to the stabilization of lanthanide metals in the liquid metals, the standard Gibbs energy changes of formation of diluted liquid alloys of lanthanides were considered to have a close-to-linear dependence on the 2/3 power of the molar volumes of the pure metals. This systematics was used to estimate those of unreported lanthanide elements. With respect to the stabilization of lanthanides and actinides in the molten alkaline salt phase, the excess free energies associated with the solution of their tri-chlorides to the alkaline chloride molten salt were estimated from the observed distribution ratios. A rough linear dependence of $\Delta G^{ex}[MCl_3$ in S] and $\Delta H^{ex}[MCl_3$ in

S] on the inverse of the ionic radius was found, and the mechanism of the stabilization of the trivalent f-element cations in the molten salt phase was deduced to be an electrostatic one. Through the correlation of the $\Delta G^{ex}[MCl_3$ in S] and ΔG_f^0[M in B] of f-elements, the stronger intermetallic interactions of lanthanides and actinides with Bi than with Zn were shown, and it was considered that actinide makes a stronger interaction with Bi than lanthanide does. We can conclude that the systematic distribution behaviors of f-elements in a pyrometallurgical bi-phase extraction system are the consequence of the thermodynamic systematics of f-elements discussed above.

A further study will be desired for elucidating more detailed mechanism of the interaction of f-element cations in the molten salt phase, and intermetallic interaction of metallic f-elements with d- and p-electron metals.

Acknowledgements

This study was supported by a Grant-in-Aid for Scientific Research of Ministry of Education, Science, Sport and Culture of Japan. Authors are indebted to Mr Sataro Nishikawa, Dr Jitsuya Takada, Mr Hisao Kodaka and Mr Kiyomi Miyata of Research Reactor Institute, Kyoto University for their technical support in the experimental activities. Authors wish to thank Mr Roy Jacobus for his help in the checking of the English expressions of this article.

References

[1] H. Moriyama, H. Yamana, S. Nishikawa, Y. Miyashita, K. Moritani, T. Mitsugashira, J. Nucl. Mater. 247 (1997) 197.
[2] H. Moriyama, H. Yamana, S. Nishikawa, S. Shibata, N. Wakayama, Y. Miyashita, K. Moritani, T. Mitsugashira, J. Alloys Compounds 271–273 (1998) 587.
[3] V.A. Lebedev, Selectivity of Liquid Metal Electrodes in Molten Halides, 1993 (in Russian).
[4] V.I. Kober, V.A. Lebedev, I.F. Nichkov, S.P. Raspopin, Russ. J. Phys. Chem. 42 (3) (1968) 360.
[5] V.I. Kober, V.A. Lebedev, I.F. Nichkov, S.P. Raspopin, Russ. J. Phys. Chem. 45 (3) (1971) 313.
[6] V.A. Lebedev, I.F. Nichkov, S.P. Raspopin, Russ. J. Phys. Chem. 42 (3) (1968) 363.
[7] I. Barin, O. Knacke, O. Kubaschewski, Thermochemical Properties of Inorganic Substances, Springer, Berlin, 1997.
[8] L.M. Ferris, J.C. Mailen, F.J. Smith, J. Inorg. Nucl. Chem. 32 (1970) 2019.
[9] L. Lumsden, Thermodynamics of Molten Salt Mixtures, Academic Press, London, 1966.
[10] F.R. DeBoer, R. Boom, W.C. Mattens, A.R. Miedema, A.K. Niessen, Cohesion in Metals–Transition Metal Alloys, North-Holland, Amsterdam, 1988.
[11] J.A. Alonso, N.H. March, Electrons in Metals and Alloys, Academic Press, London, 1989.
[12] R.D. Shannon, Acta Crystallogr. 32 (1976) 751.